Narrowband biphotons with polarization-frequency-coupled entanglement

Chi Shu, Xianxin Guo, Peng Chen, M. M. T. Loy, and Shengwang Du*

Department of Physics, The Hong Kong University of Science and Technology, Clear Water Bay, Kowloon, Hong Kong, China

(Received 21 November 2014; published 13 April 2015)

We demonstrate the generation of narrowband biphotons with polarization-frequency-coupled entanglement from spontaneous four-wave mixing in cold atoms. The coupling between polarization and frequency is realized through a frequency shifter and linear optics. When the polarization-frequency degrees of freedom are decoupled, it is robust to create polarization and frequency Bell states, confirmed by the polarization quantum-state tomography and the two-photon temporal quantum beating. Making use of the polarization-frequency coupling to transfer polarization phase retardation to the entangled frequency modes, we produce a frequency Bell state with tunable phase difference between its two bases.

DOI: 10.1103/PhysRevA.91.043820 PACS number(s): 42.50.Dv, 03.67.Bg, 03.65.Aa, 42.50.Ex

I. INTRODUCTION

Entangled photon pairs, termed *biphotons*, have become benchmark tools not only for probing fundamental quantum physics, but also for realizing applications in quantum communication and quantum computation [1]. Today, photonic entanglement can be generated in many degrees of freedom, including polarization [2–4], path (momentum) [5,6], orbital angular momentum [7], and time (frequency) [8,9]. Although entanglement is a general property of a multipartite quantum system, Bell-type entangled states are particularly important for quantum information processing and quantum teleportation [10]. For wideband biphotons generated from spontaneous parametric down conversion, Bell states of temporal entanglement can be obtained using Franson interferometry [8,9], and frequency-entangled qubits can be realized by shaping the energy spectrum [11] and polarization entanglement transfer [12]. So far, frequency Bell states for narrowband (1–50 MHz) biphotons have only been observed from spontaneous four-wave mixing (SFWM) in cold atoms [13,14]. However, in such a system, it is difficult to manipulate the frequency entanglement that is naturally endowed by energy conservation.

In this work, we demonstrate a robust scheme for generating narrowband biphotons with polarization-frequency-coupled entanglement. Narrowband single photons are particularly important for realizing efficient photon-atom quantum interfaces in a quantum network [15,16]. SFWM in laser-cooled atoms has been demonstrated as an efficient method of producing biphotons with bandwidths comparable to atomic natural linewidth (∼10 MHz) [17–21], which are of great interest for realizing efficient photon-atom quantum interfaces in a quantum network [16]. However, existing methods for generating polarization entanglement in such a system are not coupled with frequency entanglement [14,22,23]. In our simple scheme, after the generation of biphotons from SFWM, we create entanglement in both polarization and frequency simultaneously making use of an acousto-optical modulator (AOM) and linear optics. When the hyperentanglement is decoupled, we obtain controllable Bell states in either polarization or frequency modes. Our scheme can be applied to create polarization-frequency tunable entanglement from nonentangled narrowband SFWM photon pairs and may find applications in quantum communication and computation.

II. POLARIZATION-FREQUENCY-COUPLED ENTANGLEMENT: THEORY AND EXPERIMENT

Our experimental configuration is illustrated in Fig. 1(a). We produce narrowband photon pairs from SFWM in laser-cooled ^{85}Rb atoms in a three-dimensional magneto-optical trap driven by two coherent (pump and coupling) laser fields [24]. The atomic cloud has a diameter of about 1.3 mm. The relevant atomic energy levels in Fig. 1(b) are $|1\rangle = |5S_{1/2}, F = 2\rangle$, $|2\rangle = |5S_{1/2}, F = 3\rangle$, $|3\rangle = |5P_{3/2}, F = 3\rangle$, and $|4\rangle = |5P_{3/2}, F = 2\rangle$. The coupling laser ($\omega_c$, 3 mW, diameter 2 mm) is resonant to transition $|2\rangle \leftrightarrow |3\rangle$. The pump laser ($\omega_p$, 40 mW, diameter 2 mm) is far blue detuned from transition $|1\rangle \rightarrow |3\rangle$ so that the majority of the atomic population remains in the ground level $|1\rangle$. In the presence of counterpropagating pump and coupling laser beams, phase-matched backward paired Stokes (ω_s) and anti-Stokes (ω_{as}) photons are produced into two symmetric paths (1 and 2) at a right angle with respect to the pump-coupling beams: Stokes photons go to port 1 and anti-Stokes photons go to port 2, and vice versa. The atomic optical depth on the anti-Stokes transition is 5. The photons in path 1 pass through an AOM (Brimrose) and their angular frequencies are up-shifted by $\delta = 2\pi \times 100$ MHz. We collect the photons from the atomic source at the horizontal polarization with two linear polarizers. Their polarizations are later rotated to P_1 and P_2 by two half-wave ($\lambda/2$) plates. To measure the two-photon coincidence counts, the photons are coupled into two single-mode fibers that are connected to two single-photon counting modules (SPCM; Excelitas SPCM-AQRH-16-FC). Figure 1(c) shows the two-photon correlation between paths 1 and 2. The coincidence counts are collected over 3900 s and analyzed by a time-to-digital converter (Fast Comtec P7888) with a time bin width of 1 ns. Since in each photon pair the Stokes photon is always produced before its paired anti-Stokes photon and they never appear at the same time [25], we can distinguish the Stokes and anti-Stokes photons with time-resolved correlation measurement without frequency filtering. The signal at $t_2 - t_1 > 0$ represents the Stokes (path 1) to

*dusw@ust.hk

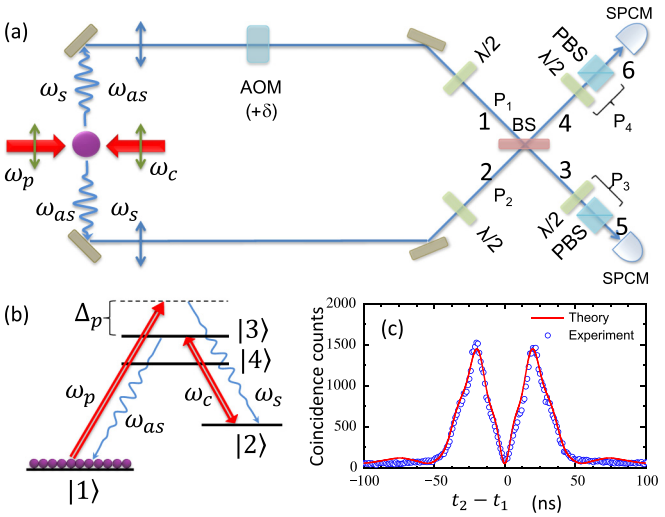

FIG. 1. (Color online) (a) Experimental schematic of narrow-band biphotons generation and detection with polarization-frequency-coupled entanglement. The photon pairs are produced from SFWM in cold ^{85}Rb atoms. (b) ^{85}Rb atomic energy level diagram. (c) Two-photon coincidence counts before the BS as a function of relative time delay between the ports 1 and 2.

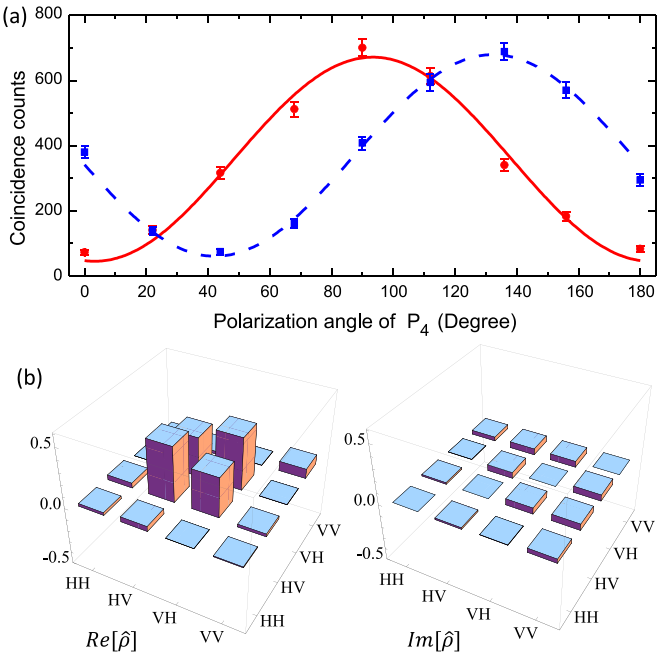

FIG. 2. (Color online) Polarization entanglement under the decoupled condition $\delta = 0$. (a) Polarization correlation between the paired photons. The coincidence counts are integrated over a 90 ns coincidence window that covers the entire biphoton wave packet. The polarization angles of the linear polarizer P_3 are fixed at 0° and −45° to the horizontal axis for the circular (red) and square (blue) experimental data, respectively. (b) Real and imaginary parts of the polarization state density matrix reconstructed from the polarization quantum-state tomography.

anti-Stokes (path 2) correlation: $G_0^{(2)}(t_2 - t_1) = |\langle t_1, t_2|\omega_s + \delta, \omega_{as}\rangle|^2 = |\psi_0(t_2 - t_1)|^2$. The signal at $t_2 - t_1 < 0$ represents the anti-Stokes (path 1) to Stokes (path 2) correlation: $G_0^{(2)}(t_1 - t_2) = |\langle t_1, t_2|\omega_{as} + \delta, \omega_s\rangle|^2 = |\psi_0(t_1 - t_2)|^2$. Here $\psi_0(\tau)$ is the Stokes–anti-Stokes biphoton relative wave form from the SFWM source. This detection postselection in relative time delay is essential for this work [26]. The experimental data in Fig. 1(c) agrees well with the theoretical curve obtained numerically following the interaction picture [13]. The biphotons have a correlation time of about 50 ns. We also perform a temporal quantum-state tomography [27] and obtain a biphoton bandwidth of about 22 MHz. To describe polarizations, we take the convention in which the wave is observed from the point of view of the source.

Paths 1 and 2 are then combined by a 50:50 beam splitter (BS). In our setup, there is no relative length difference between paths 1 and 2. The two-photon state after the BS with Stokes photon in the output port 3 and anti-Stokes photon in the output port 4 is described as

$$|\Psi_{s3,as4}\rangle = \frac{1}{\sqrt{2}}(|P_{13}, \omega_s + \delta\rangle_3 |P_{24}, \omega_{as}\rangle_4 + |P_{23}, \omega_s\rangle_3 |P_{14}, \omega_{as} + \delta\rangle_4), \quad (1)$$

where P_{ij} is the polarization state at the output port j resulted from P_i at the input port i. Setting $P_1 = H$ (horizontal polarization) and $P_2 = V$ (vertical polarization), we obtain $P_{13} = H$, $P_{14} = iH$, $P_{23} = -iV$, and $P_{24} = V$ from the BS transformation. We then get the following hyperentangled state:

$$|\Psi_{s3,as4}\rangle = \frac{1}{\sqrt{2}}(|H, \omega_s + \delta,\rangle_3 |V, \omega_{as}\rangle_4 + |V, \omega_s\rangle_3 |H, \omega_{as} + \delta\rangle_4), \quad (2)$$

where the frequency modes and polarization states are coupled together and inseparable.

To show the robustness of the scheme in entanglement manipulation, we first decouple the frequency-polarization degrees of freedom by removing the AOM from path 1, i.e., $\delta = 0$. Then the state in Eq. (2) is reduced to

$$\frac{1}{\sqrt{2}}(|HV\rangle + |VH\rangle) \otimes |\omega_s, \omega_{as}\rangle, \quad (3)$$

which is one of the polarization-entangled Bell states. To verify the polarization entanglement, we add linear polarizers P_3 and P_4 at the two BS output ports 3 and 4, respectively. Each polarizer consists of a half-wave plate and a cubic polarizing beam splitter (PBS), as shown in Fig. 1(a). The measured two-photon polarization correlations are displayed in Fig. 2(a). We take the circular (square) data points by fixing $P_3 = H$ [or $(H + V)/\sqrt{2}$] and varying the angle of P_4. The solid sinusoidal curves are the best fits with visibilities of $87 \pm 7\%$ and $84 \pm 5\%$, respectively, which violate the Bell–Clauser-Horne-Shimony-Holt (CHSH) inequality and confirm the state entanglement [28]. We further perform a polarization quantum-state tomography to fully characterize the obtained state [29,30]. To do this, we insert a quarter-wave plate before each polarizer (P_3, P_4). The density matrix is reconstructed from 16 independent coincidence counting measurements

using the maximum likelihood estimation method:

$$\begin{pmatrix} 0.02 & 0.04+0.01i & 0.00 & -0.01-0.03i \\ 0.04-0.01i & 0.46 & 0.33-0.05i & -0.02-0.05i \\ 0.00 & 0.33+0.05i & 0.44 & -0.05i \\ -0.01+0.03i & -0.02+0.05i & 0.05i & 0.08 \end{pmatrix}$$

whose graphical representation is shown in Fig. 2(b). The fidelity between the measurement and the ideal state in Eq. (3) is 88.3%. We use the obtained density matrix to test the violation of the Bell-CHSH inequality ($|S| < 2$) and obtain $S = 2.2 \pm 0.1$. Once we obtain this state, we can produce the other three independent Bell states using additional birefringent phase shifters (such as wave plates) [31]. The method demonstrated here is much simpler than that in the recent work [22], and it does not require any phase stabilization. In our setup, the main deviation of the measurement from the ideal state is caused by the imperfections of the BS and the wave plates.

We can also decouple the frequency-polarization degrees of freedom by setting $P_1 = P_2 = H$. In this case, we have $P_{13} = P_{24} = H$ and $P_{14} = P_{23} = iH$ that reduces Eq. (1) to a frequency-entangled Bell state

$$|HH\rangle \otimes \frac{1}{\sqrt{2}}(|\omega_s+\delta,\omega_{as}\rangle - |\omega_s,\omega_{as}+\delta\rangle). \quad (4)$$

The two-photon wave function in time domain can be derived as

$$\Psi(t_3,t_4) = ie^{-i(\omega_s+\delta/2)t_3}e^{-i(\omega_{as}+\delta/2)t_4}\psi_0(\tau)\sin(\delta\tau/2), \quad (5)$$

where $\tau = t_4 - t_3$. We then obtain the Glauber correlation function

$$G_{34}^{(2)}(\tau) = |\Psi(t_3,t_4)|^2 = \tfrac{1}{2}G_0^{(2)}(\tau)[1-\cos(\delta\tau)], \quad (6)$$

where $G_0^{(2)}(\tau)$ is the Stokes–anti-Stokes two-photon Glauber correlation function before the BS. Equation (6) displays a two-photon quantum beating with the frequency of $\delta/(2\pi)$ associated with the envelope of $G_0^{(2)}(\tau)$. With the two-photon joint detection efficiency η, the time-bin width Δt, and the total measurement time T, the two-photon coincidence counts can be calculated as $C_{34}(\tau) = G_{34}^{(2)}(\tau)\eta\Delta tT$. The experimental result of quantum beating is shown in Fig. 3. For comparison, we plot the two-photon coincidence counts without interference in Fig. 3(a), measured before the BS, the same as Fig. 1(c). Figure 3(b) displays the two-photon beating, as predicted from Eq. (6). To see the beating more clearly, we normalize the two-photon interference to its envelope in Fig. 3(a) and plot the normalized two-photon beating in Fig. 3(c). By best fitting the data with a sinusoidal wave we determine the visibility $V = 80 \pm 2\%$, which is far beyond the requirement for violation of Bell inequality in time-frequency domain [8].

Starting from the state in Eq. (2) and following the same procedures as Ref. [31], one can obtain the following eight independent polarization-frequency-coupled, hyperentangled quantum states by placing additional wave plates on the BS output ports 3 and 4:

$$|\Psi_{s3,as4}^{1\pm}\rangle = \frac{1}{\sqrt{2}}(|H,\omega_s+\delta\rangle_3|V,\omega_{as}\rangle_4 \pm |V,\omega_s\rangle_3|H,\omega_{as}+\delta\rangle_4), \quad (7)$$

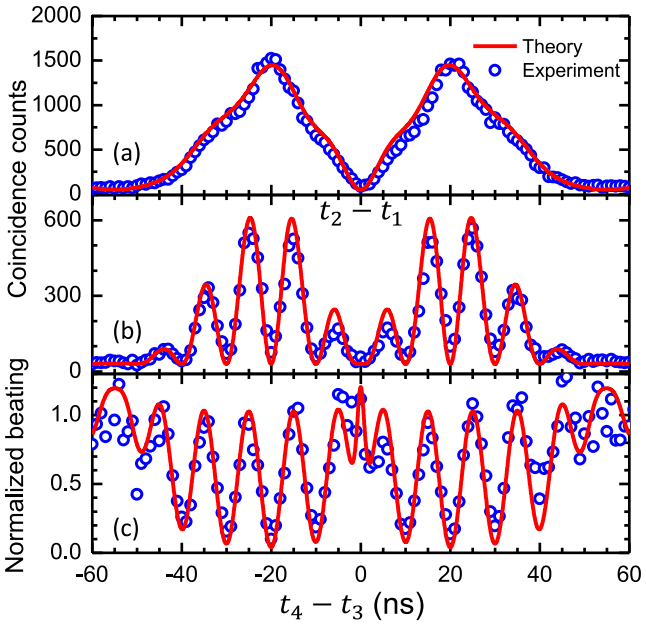

FIG. 3. (Color online) Frequency entanglement under the decoupled condition $P_1 = P_2 = P_0$. (a) Biphotons wave form before the BS. (b) Two-photon interference coincidence counts measured at the output ports 3 and 4 of the BS. (c) Normalized two-photon beating signal.

$$|\Psi_{s3,as4}^{2\pm}\rangle = \frac{1}{\sqrt{2}}(|V,\omega_s+\delta\rangle_3|H,\omega_{as}\rangle_4 \pm |H,\omega_s\rangle_3|V,\omega_{as}+\delta\rangle_4), \quad (8)$$

$$|\Phi_{s3,as4}^{1\pm}\rangle = \frac{1}{\sqrt{2}}(|H,\omega_s+\delta\rangle_3|H,\omega_{as}\rangle_4 \pm |V,\omega_s\rangle_3|V,\omega_{as}+\delta\rangle_4), \quad (9)$$

$$|\Phi_{s3,as4}^{2\pm}\rangle = \frac{1}{\sqrt{2}}(|V,\omega_s+\delta\rangle_3|V,\omega_{as}\rangle_4 \pm |H,\omega_s\rangle_3|H,\omega_{as}+\delta\rangle_4). \quad (10)$$

Exchanging Stokes and anti-Stokes photons, one can obtain another eight polarization-frequency-entangled quantum states, represented by the detection of anti-Stokes at port 3 and Stokes at port 4 ($t_4 - t_3 < 0$).

Mattle *et al.* show that the polarization birefringent effect is a powerful tool to transfer from one polarization Bell state to others with only linear optics [31]. In the following, we show that by making use of the polarization-frequency coupling we can continuously vary the relative phase between the two terms in the frequency-entangled Bell state. To achieve this, we project the hyperentangled state in Eq. (2) to the polarizers P_3 and P_4 to decouple the polarization degree of freedom from the frequency degree of freedom: $\frac{1}{\sqrt{2}}(\langle P_3|H\rangle|\langle P_4|V\rangle|\omega_s+\delta\rangle_3|\omega_{as}\rangle_4 + \langle P_3|V\rangle\langle P_4|H\rangle|\omega_s\rangle_3|\omega_{as}+\delta\rangle_4)$. We insert a quarter-wave plate before the half-wave plate in the BS output port 2 to construct a complex polarizer $P_3 = \frac{1}{\sqrt{2}}(H + e^{-i\theta}V)$. P_4 remains a linear

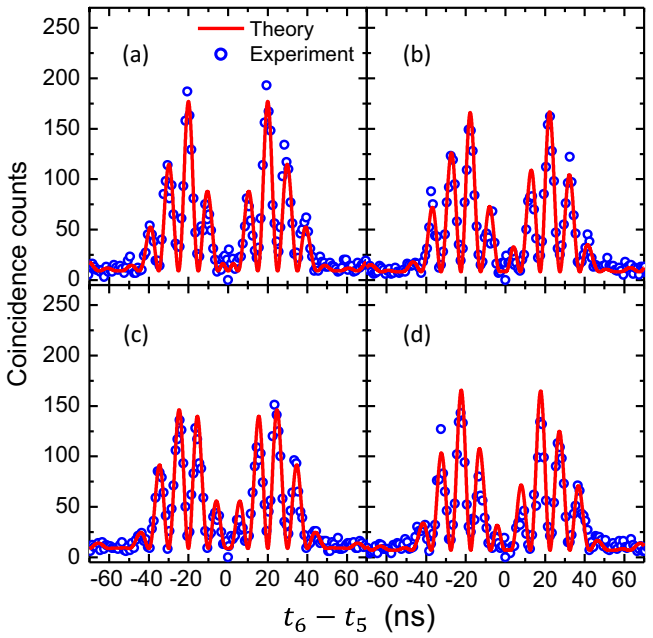

FIG. 4. (Color online) Two-photon beating for varying phase difference θ of the frequency-entangled state $\frac{1}{\sqrt{2}}\big(|\omega_s+\delta,\omega_{as}\rangle + e^{i\theta}|\omega_s,\omega_{as}+\delta\rangle\big)$: (a) $\theta=0$, (b) $\theta=\pi/2$, (c) $\theta=\pi$, and (d) $\theta=3\pi/2$.

polarizer $P_4=\frac{1}{\sqrt{2}}(H+V)$. Then the frequency-entangled state at output ports 5 and 6 [see Fig. 1(a)] is expressed as

$$\frac{1}{\sqrt{2}}(|\omega_s+\delta,\omega_{as}\rangle + e^{i\theta}|\omega_s,\omega_{as}+\delta\rangle). \tag{11}$$

The Glauber correlation function becomes

$$G^{(2)}_{56}(\tau') = \tfrac{1}{8}G^{(2)}_0(\tau')[1+\cos(\delta\tau'-\theta)], \tag{12}$$

where $\tau' = t_6 - t_5$. The factor 1/8 takes into account the BS and polarizer projection losses. The experimental results (circular data) of phase-shifted two-photon beating at different phase θ are shown in Fig. 4, agreeing well with the theory (solid curves). The visibilities of the normalized two-photon beating signal of these measurements are $77\pm5\%$, $78\pm5\%$, $80\pm4\%$, and $77\pm5\%$, for Figs. 4(a)–4(d), respectively, which are all beyond the requirement of violating the Bell-CHSH inequality.

III. SUMMARY

In summary, we demonstrate the generation of polarization-frequency-coupled entanglement for narrowband biphotons produced from the right-angle SFWM in laser-cooled atoms, making use of an AOM frequency shifter and linear optics. As the polarization-frequency degrees of freedom are decoupled, we show that the scheme is robust in creating both polarization Bell states and frequency Bell states, as confirmed by the polarization quantum-state tomography and the two-photon temporal quantum beating. Making use of this polarization-frequency coupling effect followed by a decoupling process, we can transfer the phase difference between the two polarization modes to their entangled frequency modes. We use this technique to produce the frequency-entangled Bell state whose phase difference between the two frequency bases can be continuously varied by properly adjusting the wave plates. As compared to the recent demonstration of polarization entanglement for SFWM biphotons [22], this scheme is much simpler. Moreover, we generate frequency Bell state with an AOM frequency shifter and linear optics. Our demonstration paves the way toward engineering photonic entanglements in polarization and frequency Hilbert spaces.

ACKNOWLEDGMENTS

This work was supported by the Hong Kong Research Grants Council (Project No. 16301214). C.S. acknowledges support from the Undergraduate Research Opportunities Program at the Hong Kong University of Science and Technology.

[1] J.-W. Pan, Z. B. Chen, C.-Y. Lu, H. Weinfurter, A. Zeilinger, and M. Zukowski, Multiphoton entanglement and interferometry, Rev. Mod. Phys. **84**, 777 (2012).
[2] Z. Y. Ou and L. Mandel, Violation of Bell's inequality and classical probability in a two-photon correlation experiment, Phys. Rev. Lett. **61**, 50 (1988).
[3] Y. H. Shih and C. O. Alley, New type of Einstein-Podolsky-Rosen-Bohm experiment using pairs of light quanta produced by optical parametric down conversion, Phys. Rev. Lett. **61**, 2921 (1988).
[4] P. G. Kwiat, K. Mattle, H. Weinfurter, A. Zeilinger, A. V. Sergienko, and Y. Shih, New high-intensity source of polarization-entangled photon pairs, Phys. Rev. Lett. **75**, 4337 (1995).
[5] M. A. Horne, A. Shimony, and A. Zeilinger, Two-particle interferometry, Phys. Rev. Lett. **62**, 2209 (1989).
[6] J. G. Rarity and P. R. Tapster, Experimental violation of Bell's inequality based on phase and momentum, Phys. Rev. Lett. **64**, 2495 (1990).
[7] A. Mair, A. Vaziri, G. Weihs, and A. Zeilinger, Entanglement of the orbital angular momentum states of photons, Nature (London) **412**, 313 (2001).
[8] J. D. Franson, Bell inequality for position and time, Phys. Rev. Lett. **62**, 2205 (1989).
[9] J. Brendel, N. Gisin, W. Tittel, and H. Zbinden, Pulsed energy-time entangled twin-photon source for quantum communication, Phys. Rev. Lett. **82**, 2594 (1999).
[10] M. A. Nielsen and I. L. Chuang, *Quantum Computation and Quantum Information* (Cambridge University Press, Cambridge, UK, 2000).
[11] C. Bernhard, B. Bessire, T. Feurer, and A. Stefanov, Shaping frequency-entangled qudits, Phys. Rev. A **88**, 032322 (2013).
[12] S. Ramelow, L. Ratschbacher, A. Fedrizzi, N. K. Langford, and A. Zeilinger, Discrete tunable color entanglement, Phys. Rev. Lett. **103**, 253601 (2009).
[13] S. Du, J. Wen, and M. H. Rubin, Narrowband biphoton generation near atomic resonance, J. Opt. Soc. Am. B **25**, C98 (2008).

[14] H. Yan, S. Zhang, J. F. Chen, M. M. T. Loy, G. K. L. Wong, and S. Du, Generation of narrow-band hyperentangled nondegenerate paired photons, Phys. Rev. Lett. **106**, 033601 (2011).

[15] M. Fortsch, J. U. Furst, C. Wittmann, D. Strekalov, A. Aiello, M. V. Chekhova, C. Silberhorn, G. Leuchs, and C. Marquardt, A versatile source of single photons for quantum information processing, Nat. Commun. **4**, 1818 (2013).

[16] H. J. Kimble, The quantum internet, Nature (London) **453**, 1023 (2008).

[17] V. Balic, D. A. Braje, P. Kolchin, G. Y. Yin, and S. E. Harris, Generation of paired photons with controllable waveforms, Phys. Rev. Lett. **94**, 183601 (2005).

[18] J. K. Thompson, J. Simon, H. Loh, and V. Vuletic, A high-brightness source of narrowband, identical-photon pairs, Science **313**, 74 (2006).

[19] S. Du, P. Kolchin, C. Belthangady, G. Y. Yin, and S. E. Harris, Subnatural linewidth biphotons with controllable temporal length, Phys. Rev. Lett. **100**, 183603 (2008).

[20] B. Srivathsan, G. K. Gulati, B. Chng, G. Maslennikov, D. Matsukevich, and C. Kurtsiefer, Narrow band source of transform-limited photon pairs via four-wave mixing in a cold atomic ensemble, Phys. Rev. Lett. **111**, 123602 (2013).

[21] L. Zhao, X. Guo, C. Liu, Y. Sun, M. M. T. Loy, and S. Du, Photon pairs with coherence time exceeding one microsecond, Optica **1**, 84 (2014).

[22] K. Liao, H. Yan, J. He, S. Du, Z.-M. Zhang, and S.-L. Zhu, Subnatural-linewidth polarization-entangled photon pairs with controllable temporal length, Phys. Rev. Lett. **112**, 243602 (2014).

[23] D. N. Matsukevich, T. Chaneliere, M. Bhattacharya, S.-Y. Lan, S. D. Jenkins, T. A. B. Kennedy, and A. Kuzmich, Entanglement of a photon and a collective atomic excitation, Phys. Rev. Lett. **95**, 040405 (2005).

[24] C. Liu, J. F. Chen, S. Zhang, S. Zhou, Y.-H. Kim, M. M. T. Loy, G. K. L. Wong, and S. Du, Two-photon interferences with degenerate and nondegenerate paired photons, Phys. Rev. A **85**, 021803(R) (2012).

[25] S. Du, E. Oh, J. Wen, and M. H. Rubin, Four-wave mixing in three-level systems: Interference and entanglement, Phys. Rev. A **76**, 013803 (2007).

[26] D. V. Strekalov, T. B. Pittman, A. V. Sergienko, Y. H. Shih, and P. G. Kwiat, Postselection-free energy-time entanglement, Phys. Rev. A **54**, R1(R) (1996).

[27] P. Chen, C. Shu, X. Guo, M. M. T. Loy, and S. Du, Measuring the biphoton temporal wave function with polarization-dependent and time-resolved two-photon interference, Phys. Rev. Lett. **114**, 010401 (2015).

[28] J. F. Clauser, M. A. Horne, A. Shimony, and R. A. Holt, Proposed experiment to test local hidden-variable theories, Phys. Rev. Lett. **23**, 880 (1969).

[29] A. G. White, D. F. V. James, P. H. Eberhard, and P. G. Kwiat, Nonmaximally entangled states: Production, characterization, and utilization, Phys. Rev. Lett. **83**, 3103 (1999).

[30] D. F. V. James, P. G. Kwiat, W. J. Munro, and Andrew G. White, Measurement of qubits, Phys. Rev. A **64**, 052312 (2001).

[31] K. Mattle, H. Weinfurter, P. G. Kwiat, and A. Zeilinger, Dense coding in experimental quantum communication, Phys. Rev. Lett. **76**, 4656 (1996).